Multipole structure of nucleon tensor form factors

Nam-Yong Ghim,[1,*] Ho-Yeon Won,[2,†] June-Young Kim,[1,2,‡] and Hyun-Chul Kim[1,3,§]

[1]*Department of Physics and Institute of Quantum Science, Inha University, Incheon 22212, Republic of Korea*

[2]*CPHT, CNRS, École polytechnique, Institut Polytechnique de Paris, Palaiseau, France*

[3]*School of Physics, Korea Institute for Advanced Study (KIAS), Seoul 02455, Republic of Korea*

(Received 26 May 2026; accepted 1 July 2026; published 10 August 2026)

We investigate the multipole structure of nucleon tensor form factors within the chiral quark-soliton model based on the $1/N_c$ expansion. Extending the previous leading-order analysis [N.-Y. Ghim *et al.*, Phys. Rev. D **111**, 074024 (2025)], we include the rotational $1/N_c$ corrections. These corrections provide the leading nonvanishing contributions to the flavor components that are absent at leading order, thereby completing the flavor decomposition of the tensor multipole form factors at the present order. We numerically evaluate the isoscalar tensor charge, the isovector anomalous tensor magnetic moment, and the isoscalar tensor quadrupole moment, obtaining $g_T^{u+d} = 0.81$, $\kappa_T^{u-d} = 1.97$, and $E_T^{u+d}(0) = 5.98$, respectively. The isoscalar tensor charge and quadrupole moment are mainly governed by the valence-quark contribution, whereas the isovector anomalous tensor magnetic moment receives a sizable Dirac-sea contribution. We also examine the momentum-transfer dependence of the corresponding form factors. They decrease monotonically with increasing $-t$. In particular, the isovector anomalous tensor magnetic form factor shows a pronounced falloff in the small-$|t|$ region, reflecting the importance of the Dirac sea in the tensor dipole structure.

DOI: 10.1103/wtdr-92yh

I. INTRODUCTION

The tensor charges of the nucleon carry several significant physical implications, which are defined as the forward nucleon matrix elements of the tensor bilinear quark operators [1–4]. For example, they are essential for probing new physics through precision β-decay experiments and for setting limits on the neutron electric dipole moment beyond the Standard Model [5–12]. They also play an important role in the interactions of dark matter with the nucleon [12–18]. Originally, the flavor-singlet tensor charge was introduced as the first Mellin moment of the transversity parton distribution function (PDF) $h_1(x)$ [2,3], which provides essential information on the spin structure of the nucleon [2,3,19–23] (see also the reviews [24–26]).

While the leading-twist unpolarized PDF $f_1(x)$ and the longitudinally polarized PDF $g_1(x)$ can be measured in deep-inelastic scattering [27,28], the third leading-twist distribution, the transversely polarized PDF $h_1(x)$, is inaccessible in inclusive deep-inelastic scattering. Instead, it can be extracted from processes such as the transverse spin asymmetry A_{TT} in Drell-Yan $p\bar{p}$ reactions [29–32] and in semi-inclusive deep-inelastic scattering (SIDIS) at HERMES and COMPASS [33–36]. More refined extractions were performed in Refs. [37,38] by combining SIDIS data with the Collins fragmentation function [39] measured by the Belle Collaboration [40]. Since then, additional empirical information on the tensor charges has been obtained [41–46]. Moreover, increasingly precise lattice QCD results have been accumulated over several decades [47–57].

The chiral-odd generalized parton distributions (GPDs) broaden the physical meaning of the tensor charges and related form factors [58–65], since they encode information on both PDFs and form factors. In particular, the tensor form factors arise as the first Mellin moments of the chiral-odd GPDs. As discussed in Refs. [2,3], the flavor-singlet tensor charge counts valence quarks (quarks minus antiquarks) of opposite transversity. Notably, sea quarks do not contribute because the tensor bilinear quark operator is odd under charge conjugation. In contrast, the axial-vector operator is even under charge conjugation, so the axial charge receives contributions from sea-quark helicities. At leading twist, there are four chiral-odd GPDs [58,59].

[*]Contact author: Namyong.ghim@inha.edu
[†]Contact author: hoyeon.won@polytechnique.edu
[‡]Contact author: jun-young.kim@inha.ac.kr
[§]Contact author: hchkim@inha.ac.kr

However, only three independent first Mellin moments survive, since one of the GPDs vanishes upon integration over the Bjorken variable x. These three moments correspond to the independent multipole tensor form factors. In the forward limit, the first becomes the tensor charge δq for quark flavor q. The second is the tensor anomalous magnetic dipole moment κ_T^q, which characterizes the deformation of the average transverse position of quarks polarized in the transverse direction relative to the transverse center of light-front momentum for an unpolarized target [66]. In Refs. [48,67], the transverse spin structure of the nucleon was further explored using chiral-odd GPDs. In this context, the final tensor form factor Q_T^q was identified with the tensor quadrupole moment, which characterizes the quadrupole distortion of the transverse spin density in the polarized nucleon. These chiral-odd GPDs and tensor form factors have been studied within various theoretical approaches, including constituent quark models in the light-cone basis [68,69], MIT bag models [4,70], light-front quark models [71,72], light-cone quark models [73], and QCD sum rules [74].

They have also been studied in the chiral quark-soliton model (χQSM) [75–84]. In our previous work [75], we revisited the tensor form factors, ensuring consistency between the chiral-odd GPDs [83] and the tensor form factors in the large-N_c limit of QCD. We elaborated on the anomalous tensor magnetic dipole moments studied in Refs. [81,82], and we computed the leading contribution to the tensor quadrupole moment Q_T in the large-N_c limit. This quantity is as important as the tensor charge and the anomalous tensor magnetic dipole moment, since it is also related to the leading-twist chiral-odd GPD $\tilde{H}_T$.

This work extends the investigation of Ref. [75] by including rotational $1/N_c$ corrections [84] within the framework of the χQSM. The model has the distinctive advantage that it satisfies the polynomiality of the chiral-odd GPDs and various sum rules in the large-N_c limit of QCD [83]. The χQSM incorporates chiral symmetry and its spontaneous breaking in QCD, which can be derived from the instanton vacuum [85–88] (see Refs. [89,90] for reviews). The instanton vacuum is characterized by two parameters, namely the average instanton size $\bar{\rho} \approx 1/3$ fm and the mean separation between instantons (and anti-instantons) $\bar{R} \approx 1$ fm. It generates localized quark zero modes with definite chirality, which subsequently become delocalized and undergo chirality flips as quarks propagate through the instanton–anti-instanton medium. As a result, the quarks acquire a dynamical mass and the pseudo–Nambu-Goldstone bosons emerge, realizing the spontaneous breaking of chiral symmetry (SBχS). Furthermore, this picture introduces the instanton packing fraction as a small parameter, enabling a systematic expansion for studying SBχS and hadronic correlation functions. Effective dynamics at the scale $\bar{R}$ can be constructed using $1/N_c$ expansion techniques, including the saddle-point approximation and bosonization. This leads to a description in which quarks with a dynamical mass $M \sim 0.3$–0.4 GeV interact with a chiral pion field. Within this framework, the nucleon emerges as a bound state of N_c valence quarks in a self-consistent mean field [91]. Thus, the χQSM provides a concrete realization of the baryon picture in large-N_c QCD [92,93]. This effective chiral theory for the nucleon has been very successful in describing many nucleon observables (see Ref. [94] for a review). The model can also describe low-lying singly heavy baryons on the same footing [95–98].

This work is organized as follows. We first set up the general formalism of the tensor form factors in Sec. II, where the multipole expansion is performed in the Breit frame. After briefly reviewing the basic ingredients of the χQSM in Sec. III, we apply the model to the tensor form factors and derive the relevant expressions in Sec. IV. The numerical results are then presented and discussed in Sec. V. Finally, Sec. VI summarizes the main findings and gives the conclusions.

II. TENSOR FORM FACTORS

The quark tensor operator is defined by

$$O_q^{\mu\nu}(x) = \bar{\psi}_q(x) i\sigma^{\mu\nu}\psi_q(x), \tag{1}$$

where ψ_q is the quark field operator of flavor $q = u, d, \cdots$, and $\sigma^{\mu\nu} = i[\gamma^\mu, \gamma^\nu]/2$. We denote the matrix element of the tensor operator as

$$\mathcal{M}^q[i\sigma^{\mu\nu}] = \langle N(p', S_3')|O_q^{\mu\nu}(0)|N(p, S_3)\rangle, \tag{2}$$

where p and p' are, respectively, the initial and final nucleon four momenta, and S_3 and S_3' are the corresponding spin projections. The nucleon states are normalized as

$$\langle N(p', S_3')|N(p, S_3)\rangle = (2\pi)^3 2p^0 \delta_{S_3' S_3} \delta^{(3)}(\boldsymbol{p}' - \boldsymbol{p}). \tag{3}$$

Then Eq. (2) can be parametrized in terms of the tensor form factors

$$\mathcal{M}^q[i\sigma^{\mu\nu}] = \bar{u}\left[H_T^q i\sigma^{\mu\nu} + \tilde{H}_T^q \frac{P^\mu\Delta^\nu - P^\nu\Delta^\mu}{M_N^2} + E_T^q \frac{\gamma^\mu\Delta^\nu - \gamma^\nu\Delta^\mu}{2M_N}\right]u, \tag{4}$$

where $u \equiv u(p, S_3)$ and $\bar{u} \equiv \bar{u}(p', S_3')$. The average momentum and momentum transfer are defined by

$$P = \frac{p' + p}{2}, \qquad \Delta = p' - p. \tag{5}$$

For on-shell nucleons, $p'^2 = p^2 = M_N^2$, they obey

$$P\cdot\Delta = 0, \qquad P^2 + \frac{\Delta^2}{4} = M_N^2, \tag{6}$$

where M_N is the nucleon mass. The form factors $F^q \equiv F^q(t)$, with $F = H_T, \tilde{H}_T, E_T$, are functions of $t = \Delta^2$; their dependence on the renormalization scale is understood and not displayed explicitly.

We work in the three-dimensional (3D) Breit frame (BF), where the average momentum and momentum transfer are given by

$$P = (P^0, \mathbf{0}), \qquad \Delta = (0, \boldsymbol{\Delta}), \tag{7}$$

with $(P^0)^2 = M_N^2 - t/4$ following from the on-shell constraint (6). In this frame, the matrix element (4) can be expanded in terms of irreducible tensors constructed from $\boldsymbol{\Delta}$,

$$\mathcal{M}^q[i\sigma^{0k}] = \mathbf{1}\, Y_1^k \sqrt{-t}\left[H_T^q + E_T^q + \frac{2(P^0)^2}{M_N^2}\tilde{H}_T^q\right], \tag{8a}$$

$$\begin{aligned}\mathcal{M}^q[i\sigma^{ij}] =& 2M_N i\epsilon^{ijk}\sigma^k Y_0 \\ &\times\left[\left(\frac{P^0}{3M_N}+\frac{2}{3}\right)H_T^q + \frac{t}{6M_N^2}E_T^q\right] \\ &- i\epsilon^{ijk}\sigma^m Y_2^{km}\frac{t}{2M_N}\left[\frac{M_N}{P^0+M_N}H_T^q + E_T^q\right].\end{aligned} \tag{8b}$$

Here the rank-n irreducible tensors are defined as

$$Y_0 = 1, \qquad Y_1^i = \frac{\Delta^i}{|\boldsymbol{\Delta}|}, \qquad Y_2^{ij} = \frac{\Delta^i\Delta^j}{\boldsymbol{\Delta}^2} - \frac{1}{3}\delta^{ij}, \tag{9}$$

where the spatial indices run over i, $j = 1, 2, 3$, and

$$\mathbf{1} \equiv \delta_{S_3' S_3}, \qquad \boldsymbol{\sigma} \equiv \boldsymbol{\sigma}_{S_3' S_3} \tag{10}$$

denote the identity matrix and the Pauli matrices between the initial and final spin states, respectively.

Equation (8) exhibits three independent tensor multipole structures. We define the corresponding 3D tensor multipole moments by the form-factor combinations at $t = 0$ [75]:

$$\text{Monopole:}\ H_T^q(0), \tag{11a}$$

$$\text{Dipole:}\ H_T^q(0) + E_T^q(0) + 2\tilde{H}_T^q(0), \tag{11b}$$

$$\text{Quadrupole:}\ \frac{1}{2}H_T^q(0) + E_T^q(0). \tag{11c}$$

For comparison, the corresponding two-dimensional tensor multipole moments are defined in Ref. [75] as

$$\text{Monopole:}\ H_T^q(0) = g_T^q, \tag{12a}$$

$$\text{Dipole:}\ E_T^q(0) + 2\tilde{H}_T^q(0) = \kappa_T^q, \tag{12b}$$

$$\text{Quadrupole:}\ 2\tilde{H}_T^q(0) = Q_T^q. \tag{12c}$$

III. CHIRAL QUARK-SOLITON MODEL

In this section, we briefly review the χQSM, an effective theory for baryons, and show how the tensor form factors can be evaluated within this framework. The low-energy effective QCD partition function is written in Euclidean space as

$$\begin{aligned}\mathcal{Z}_{\text{eff}} &= \int D\psi D\psi^\dagger\, DU\, \exp\left[\int d^4x \psi^\dagger D(U)\psi\right] \\ &= \int DU\, \exp\left(-S_{\text{eff}}[U]\right),\end{aligned} \tag{13}$$

with the single-particle Dirac operator defined as

$$D(U) = i\partial + iMU^{\gamma_5} + i\hat{m}. \tag{14}$$

Integrating out the quark fields in Eq. (13), we derive the effective chiral action

$$S_{\text{eff}}[U] = -N_c \operatorname{Tr}\ln D(U). \tag{15}$$

Here M, $\hat{m}$, and U denote the dynamical quark mass, the current-quark mass matrix, and the chiral field, respectively. In the instanton vacuum, the dynamical quark mass is momentum dependent, $M(k)$, owing to the finite average instanton size $\bar{\rho}$. The instanton form factor suppresses quark modes with $k \gtrsim \bar{\rho}^{-1}$, so that $\bar{\rho}^{-1}$ sets the natural ultraviolet scale of the effective theory. In the present work, we use a constant mass $M(k) = M(0) \equiv M$ and implement this scale through the proper-time regularization. The cutoff mass is identified approximately with a scale of order $\bar{\rho}^{-1}$. The current-quark mass matrix is given as

$$\hat{m} = \text{diag}(m_u, m_d), \tag{16}$$

and isospin symmetry is assumed, $m_u = m_d = m$.

The chiral field U is an SU(2) matrix field containing the pion fields. It is defined as

$$U^{\gamma_5} = \frac{1+\gamma_5}{2}U + \frac{1-\gamma_5}{2}U^\dagger, \tag{17a}$$

$$U = \exp\left(i\pi^a\tau^a\right), \tag{17b}$$

where π^a denote the pion fields and τ^a represent the Pauli matrices in flavor space. To describe a baryon, we use a static pion field with hedgehog symmetry,

$$U^{\gamma_5}(\boldsymbol{x}) = \exp\left[i\gamma_5 \boldsymbol{n}\cdot\boldsymbol{\tau}P(r)\right], \tag{18}$$

where $r = |\boldsymbol{x}|$ and $n^a = x^a/r$, and the Euclidean γ_5 matrix is $\gamma_5 \equiv \gamma_1\gamma_2\gamma_3\gamma_4$. Equivalently, the pion field has the form $\pi^a(\boldsymbol{x}) = n^a P(r)$, where $P(r)$ is a radial profile function satisfying $P(0) = \pi$ and $P(\infty) = 0$. In this ansatz, the isospin direction of the pion field is identified with the radial direction in coordinate space.

From Eq. (14), the single-particle Dirac Hamiltonian is obtained as

$$H(U) = \gamma_4\gamma_k\partial_k + \gamma_4 M U^{\gamma_5} + \gamma_4\hat{m}. \tag{19}$$

Because of the hedgehog symmetry, the Hamiltonian is invariant under combined rotations generated by the total angular momentum $\boldsymbol{J} = \boldsymbol{L} + \boldsymbol{S}$ and the isospin $\boldsymbol{T}$. The generator of this combined rotation is the grand spin,

$$\boldsymbol{G} = \boldsymbol{J} + \boldsymbol{T}, \tag{20}$$

where $\boldsymbol{L}$ and $\boldsymbol{S}$ are the orbital angular momentum and quark spin operators. Hence $[H(U), \boldsymbol{G}] = 0$, and the single-particle eigenstates can be classified by the grand-spin quantum number.

The single-particle eigenfunctions and eigenenergies are determined from

$$H(U)\Phi_n(\boldsymbol{x}) = E_n\Phi_n(\boldsymbol{x}), \quad \text{with} \quad \Phi_n(\boldsymbol{x}) \equiv \langle \boldsymbol{x}|n\rangle, \tag{21}$$

where the label n collectively denotes the quantum numbers

$$n = \{G, G_3, \Pi, \ldots\}. \tag{22}$$

Here G and G_3 stand for the grand spin and its projection, respectively, Π is the parity, and the ellipsis denotes the remaining radial quantum number. The single-particle energies associated with these states form the Dirac spectrum in the chiral background field. This field polarizes the positive- and negative-energy continua and, for a sufficiently strong field, produces a discrete bound level

$$|\text{lev}\rangle \equiv |n = \{E_{\text{lev}}, G = 0, G_3 = 0, \Pi = +\}\rangle \tag{23}$$

with $-M < E_{\text{lev}} < M$. Occupying this bound level with the N_c valence quarks with the negative-energy Dirac continuum (or Dirac sea) yields the ground-state baryon with baryon number $B = 1$. Then the classical energy is obtained by

$$E_{\text{cl}}[U] = N_c E_{\text{lev}}[U] + E_{\text{sea}}[U]. \tag{24}$$

Here the first term comes from the occupied bound level, whereas E_{sea} denotes the regularized and vacuum-subtracted contribution of the filled negative-energy continuum.

In the large-N_c limit, the functional integral over U is dominated by the configuration that minimizes $E_{\text{cl}}[U]$. This stationary configuration defines the self-consistent pion mean field U_{cl},

$$\left.\frac{\delta E_{\text{cl}}[U]}{\delta U}\right|_{U=U_{\text{cl}}} = 0. \tag{25}$$

Evaluating the energy functional at this field, we obtain the classical nucleon mass

$$M_{\text{cl}} = E_{\text{cl}}[U_{\text{cl}}]. \tag{26}$$

Details of the self-consistent construction are given in Ref. [94].

Corrections beyond the leading order in the large-N_c expansion arise from $1/N_c$ quantum fluctuations of the pion field around the self-consistent field U_{cl}, which are neglected. The translational and rotational zero modes must be considered completely. This will assign proper quantum numbers for the nucleon. Thus, the collective Hamiltonian is obtained as

$$H_{\text{rot}} = \frac{\hat{\boldsymbol{S}}^2}{2I} = \frac{\hat{\boldsymbol{T}}^2}{2I}, \tag{27}$$

where $\hat{\boldsymbol{S}}$ and $\hat{\boldsymbol{T}}$ are the spin and isospin operators. The moment of inertia is expressed as

$$I = \frac{N_c}{6}\sum_{\substack{n,\text{occ}\\ m,\text{non}}} \frac{\langle n|\tau^a|m\rangle\langle m|\tau^a|n\rangle}{E_m - E_n}. \tag{28}$$

Here the sum runs over occupied levels n and nonoccupied levels m of the Dirac Hamiltonian (19). Since $I = O(N_c)$, the rotational Hamiltonian is $H_{\text{rot}} = O(1/N_c)$ and therefore gives a subleading correction to the nucleon mass.

Because of the hedgehog symmetry, the collective Hamiltonian (27) has the form of a spherical top. The baryon collective wave functions are therefore its eigenfunctions and can be written as Wigner D-functions carrying the spin and isospin quantum numbers of the quantized classical nucleon. The explicit representation is given in Ref. [94].

IV. TENSOR FORM FACTORS IN THE CHIRAL QUARK-SOLITON MODEL

The nucleon matrix element of the tensor current can be derived from the three-point correlation function,

$$\begin{aligned}
&\langle N(p', S_3')|O^{\mu\nu}_{q,\mathrm{E}}(0)|N(p,S_3)\rangle \\
&= \frac{1}{Z_{\mathrm{eff}}}\lim_{\mathrm{T}\to\infty}\exp\left(-ip_4\frac{T}{2}-ip_4'\frac{T}{2}\right) \\
&\quad\times\int d^3\boldsymbol{x}d^3\boldsymbol{y}\exp(-i\boldsymbol{p}'\cdot\boldsymbol{y}+i\boldsymbol{p}\cdot\boldsymbol{x}) \\
&\quad\times\int\mathcal{D}\psi\mathcal{D}\psi^\dagger\mathcal{D}UJ_N(\boldsymbol{y},T/2)O^{\mu\nu}_{q,\mathrm{E}}(0)J_N(\boldsymbol{x},-T/2) \\
&\quad\times\exp\left[\int d^4z\psi^\dagger(z)D(U)\psi(z)\right],
\end{aligned}\tag{29}$$

where $O^{\mu\nu}_{q,\mathrm{E}}$ is the Euclidean counterpart of the tensor operator defined in Eq. (1). The nucleon Ioffe-type current J_N consists of the N_c valence quarks

$$J_N(x)=\frac{1}{N_c!}\epsilon_{\alpha_1\cdots\alpha_{N_c}}\Gamma^{\beta_1\cdots\beta_{N_c}}_{SS_3TT_3}\psi_{\alpha_1\beta_1}(x)\cdots\psi_{\alpha_{N_c}\beta_{N_c}}(x),\tag{30}$$

where α_i and β_i denote color and spin-flavor indices, respectively. The matrices $\Gamma^{\beta_1\cdots\beta_{N_c}}_{SS_3TT_3}$ carry quantum numbers such as spin S, isospin T, and third components S_3 and T_3 for the nucleon.

We decompose the tensor-current matrix element computed in the χQSM into isoscalar and isovector components. In the strict large-N_c limit, its spin-flavor structure selects only the leading flavor components: the isoscalar part of $\mathcal{M}^{u+d}[i\sigma^{0k}]$ and the isovector part of $\mathcal{M}^{u-d}[i\sigma^{ij}]$. The complementary components vanish at this order; see Ref. [75] for details. They are generated once the rotational zero modes are quantized. Although the corresponding rotational corrections are subleading in the $1/N_c$ expansion, they give the leading nonvanishing contributions to $\mathcal{M}^{u-d}[i\sigma^{0k}]$ and $\mathcal{M}^{u+d}[i\sigma^{ij}]$. Thus they complete the flavor decomposition of the tensor-current matrix element beyond the strict large-N_c limit.

After evaluating the Euclidean correlation function in Eq. (29), we convert the resulting matrix element from Euclidean to Minkowski conventions before matching it to the tensor form-factor decomposition in Eq. (8). The large-N_c scaling of the kinematic variables entering the matrix element is

$$\Delta^0=\mathcal{O}(N_c^{-1}),\qquad \boldsymbol{\Delta}=\mathcal{O}(N_c^0),\tag{31a}$$

$$P^0=\mathcal{O}(N_c^1),\qquad \boldsymbol{P}=\mathcal{O}(N_c^0),\tag{31b}$$

with $t=\mathcal{O}(N_c^0)$. In our analysis, the nucleon mass is identified with the classical nucleon mass up to rotational corrections,

$$M_N=M_{\mathrm{cl}}+\mathcal{O}(N_c^{-1}).\tag{32}$$

Keeping this hierarchy, we organize the rotational contributions in terms of mean-field form factors in the 3D BF

$$\mathcal{M}^{u-d}[i\sigma^{0k}]=Y_1^k\,\mathbf{1}\sqrt{-t}F^{u-d}_{\mathrm{mf},1},\tag{33a}$$

$$\begin{aligned}\mathcal{M}^{u+d}[i\sigma^{ij}]&=i\epsilon^{ijk}\sigma^k\,2\,M_{\mathrm{cl}}\,Y_0F^{u+d}_{\mathrm{mf},0}\\&\quad-i\epsilon^{ijk}\sigma^mY_2^{km}\frac{t}{2M_{\mathrm{cl}}}F^{u+d}_{\mathrm{mf},2}.\end{aligned}\tag{33b}$$

Here $F_{\mathrm{mf},0}$, $F_{\mathrm{mf},1}$, and $F_{\mathrm{mf},2}$ denote mean-field form factors, with their dependence on t suppressed for brevity. The resulting multipole structures are consistent with the general decomposition in Eq. (8).

The matching must be performed with the large-N_c hierarchy of both the kinematic factors (31) and the tensor form factors kept consistently. The tensor form factors scale as [75]

$$\{H_T^{u-d},E_T^{u-d},\tilde{H}_T^{u-d}\}\sim\{N_c^1,N_c^3,N_c^3\},\tag{34a}$$

$$\{H_T^{u+d},E_T^{u+d},\tilde{H}_T^{u+d}\}\sim\{N_c^0,N_c^2,N_c^2\}.\tag{34b}$$

We then relate the mean-field form factors to the tensor form factors by matching Eq. (33) to the general decomposition in Eq. (8). This gives

$$H_T^{u+d}+\frac{t}{6M_N^2}E_T^{u+d}=F^{u+d}_{\mathrm{mf},0},\tag{35a}$$

$$H_T^{u-d}+E_T^{u-d}+2\tilde{H}_T^{u-d}=F^{u-d}_{\mathrm{mf},1},\tag{35b}$$

$$E_T^{u+d}=F^{u+d}_{\mathrm{mf},2}.\tag{35c}$$

It is worth noting that the relation in Eq. (35b) reflects a nontrivial large-N_c cancellation. In the large-N_c limit, the leading parts of E_T^{u-d} and $2\tilde{H}_T^{u-d}$ cancel each other, following the relation $E_T^{u-d}=-2\tilde{H}_T^{u-d}$ up to subleading corrections [75,83]. As a result, the combination $H_T^{u-d}+E_T^{u-d}+2\tilde{H}_T^{u-d}$ has a reduced large-N_c scaling, which leads to $F^{u-d}_{\mathrm{mf},1}=O(N_c)$.

With the above relations in mind, we use the mean-field form factors as the basis for the following analysis. Their explicit expressions are obtained as

$$\begin{aligned}F^{u+d}_{\mathrm{mf},0}(t)&=-\frac{N_c}{6I}\sum_{\substack{n,\mathrm{non}\\m,\mathrm{occ}}}\frac{\langle n|\tau^l|m\rangle}{E_n-E_m}\\&\quad\times\langle m|\Sigma^l\gamma^0j_0(|\hat{\boldsymbol{x}}|\sqrt{-t})|n\rangle,\end{aligned}\tag{36a}$$

$$\begin{aligned}F^{u-d}_{\mathrm{mf},1}(t)&=-\frac{iM_{\mathrm{cl}}N_c}{3I\sqrt{-t}}\sum_{\substack{n,\mathrm{non}\\m,\mathrm{occ}}}\frac{\langle n|\tau^l|m\rangle}{E_n-E_m}\\&\quad\times\langle m|j_1(|\hat{\boldsymbol{x}}|\sqrt{-t})Y_1^k\left(\frac{\hat{\boldsymbol{x}}}{|\hat{\boldsymbol{x}}|}\right)\gamma^k\tau^l|n\rangle,\end{aligned}\tag{36b}$$

$$F^{u+d}_{\mathrm{mf},2}(t) = -\frac{3M_{\mathrm{cl}}^2 N_c}{It}\sum_{\substack{n,\mathrm{non}\\ m,\mathrm{occ}}}\frac{\langle n|\tau^l|m\rangle}{E_n - E_m} \times \langle m|j_2(|\hat{\boldsymbol{x}}|\sqrt{-t})Y_2^{lk}\left(\frac{\hat{\boldsymbol{x}}}{|\hat{\boldsymbol{x}}|}\right)\Sigma^k\gamma^0|n\rangle. \tag{36c}$$

Here $\Sigma^k = \gamma^0\gamma^5\gamma^k$, and $\hat{\boldsymbol{x}}$ denotes the position operator. The function $j_L(|\hat{\boldsymbol{x}}|\sqrt{-t})$ is the spherical Bessel function, and the irreducible tensors appearing in Eq. (36) are defined in position space. The single-particle sums contain both the discrete-level and Dirac-sea contributions. The discrete-level contribution is obtained by restricting the occupied-state sum over m to the bound level specified in Eq. (23).

To obtain the spatial representation of the mean-field form factors, we insert the coordinate-space completeness relation into Eq. (36). We define $\rho^{u+d}_{T0}(r)$, $\rho^{u-d}_{T1}(r)$, and $\rho^{u+d}_{T2}(r)$ through

$$F^{u+d}_{\mathrm{mf},0}(t) = \int d^3r\, j_0(r\sqrt{-t})\rho^{u+d}_{T0}(r), \tag{37a}$$

$$F^{u-d}_{\mathrm{mf},1}(t) = 3\int d^3r \frac{j_1(r\sqrt{-t})}{r\sqrt{-t}}\rho^{u-d}_{T1}(r), \tag{37b}$$

$$F^{u+d}_{\mathrm{mf},2}(t) = 15\int d^3r \frac{j_2(r\sqrt{-t})}{(r\sqrt{-t})^2}\rho^{u+d}_{T2}(r). \tag{37c}$$

Their explicit expressions are given in the Appendix. These distributions are normalized so that their 3D integrals yield the corresponding tensor multipole moments,

$$F^{u+d}_{\mathrm{mf},0}(0) = \int d^3r\,\rho^{u+d}_{T0}(r) = g^{u+d}_T, \tag{38a}$$

$$F^{u-d}_{\mathrm{mf},1}(0) = \int d^3r\,\rho^{u-d}_{T1}(r) = \kappa^{u-d}_T + g^{u-d}_T, \tag{38b}$$

$$F^{u+d}_{\mathrm{mf},2}(0) = \int d^3r\,\rho^{u+d}_{T2}(r) = E^{u+d}_T(0). \tag{38c}$$

V. NUMERICAL RESULTS AND DISCUSSION

We are now in a position to present the numerical results for the tensor form factors and their moments and to discuss them. We first specify the model parameters used in the self-consistent calculation. The dynamical quark mass is taken to be $M = 350$ MeV, as motivated by the instanton-vacuum picture of QCD [90]. We employ the proper-time regularization scheme, in which the cutoff mass Λ and the current quark mass m are fixed by reproducing the experimental values of the pion decay constant $f_\pi = 93$ MeV and the pion mass $m_\pi = 140$ MeV, respectively. This yields

$$\Lambda = 643\ \mathrm{MeV}, \qquad m = 16\ \mathrm{MeV}. \tag{39}$$

Further details of the parameter fixing are given in Ref. [94].

With these parameters, we solve the Dirac eigenvalue problem in Eq. (19) using the Kahana-Ripka method [99]. The classical energy functional constructed from the resulting spectrum is minimized to determine the self-consistent pion mean field. Evaluating the energy at this minimum yields the classical nucleon mass,

$$M_{\mathrm{cl}} = 1254\ \mathrm{MeV}. \tag{40}$$

The same finite-box basis is used to evaluate the tensor form factors. In our previous work [75], a spherical box of radius $D = 11$ fm was sufficient. In the present calculation, however, $E^{u+d}_T(0)$ is sensitive to the large-distance region. We therefore increase the box size to $D = 56$ fm to ensure numerical convergence. The resulting tensor moments are listed in Table I and are compared with those from other models in Table II. As shown in Table I, the discrete level provides the dominant contribution to the isoscalar tensor charge, $g^{u+d}_T[\mathrm{lev}] = 0.78$, whereas the Dirac sea contributes only marginally, $g^{u+d}_T[\mathrm{sea}] = 0.03$. The latter amounts to

TABLE I. Numerical results for the isoscalar tensor charge g^{u+d}_T, the isovector tensor anomalous magnetic moment κ^{u-d}_T, and the isoscalar 3D tensor quadrupole moment $E^{u+d}_T(0)$ of the nucleon. The results are obtained with $M = 350$ and $m_\pi = 140$ MeV.

	Level	Dirac sea	Total
g^{u+d}_T	0.78	0.03	0.81
κ^{u-d}_T	1.56	0.41	1.97
$E^{u+d}_T(0)$	5.66	0.32	5.98

TABLE II. The mean-field results for the tensor form factors compared with those from lattice QCD [10,52,55], the bag model [4,70,100], the light-front constituent quark model (CQM) [68], and QCD sum rules [101]. For the lattice calculations, Alexandrou *et al.* [52,55] used the physical pion mass, whereas Bhattacharya *et al.* [10] used ensembles with $m_\pi = 130$, 220, and 310 MeV.

	g^{u+d}_T	κ^{u-d}_T	E^{u+d}_T
This work	0.81	1.97	5.98
Lattice QCD [52]	0.563 ± 0.026	…	…
Lattice QCD [10]	0.541 ± 0.067	…	…
Lattice QCD [55]	…	1.051 ± 0.094	…
Bag model [100]	0.80	…	…
Bag model [4]	0.88	…	…
Bag model [70]	0.82 ± 0.12	…	3.7
CQM [68] (HO)	…	1.24	…
CQM [68] (HYP)	…	0.81	…
Sum rule [101]	…	1.82	…

only about 2%–3% of the total value, $g_T^{u+d} = 0.81$. This result is close to the MIT bag-model estimates, $g_T^{u+d} = 0.88$ [4], $g_T^{u+d} = 0.80$ [100], and $g_T^{u+d} = 0.82$ [70]. Since the bag model is based mainly on valence-quark degrees of freedom, this agreement supports the dominance of the valence contribution to the isoscalar tensor charge. Lattice QCD calculations give smaller values, $g_T^{u+d} = 0.563 \pm 0.026$ [52] and $g_T^{u+d} = 0.541 \pm 0.067$ [10]. The present result is larger than these values by about 30%. In the current calculation, however, the isoscalar tensor charge is evaluated at the leading nonvanishing order in the $1/N_c$ expansion. The discrepancy may therefore be attributed, at least in part, to subleading $1/N_c$ corrections.

For the isovector tensor anomalous magnetic moment, the discrete-level contribution is $\kappa_T^{u-d}[\mathrm{lev}] = 1.56$, while the Dirac-sea contribution is $\kappa_T^{u-d}[\mathrm{sea}] = 0.41$. The latter accounts for about 21% of the total value and is therefore sizable compared with the sea contributions to the other tensor moments. This sizable sea contribution can be traced to the chiral structure of the corresponding tensor operator, which differs from those of the other tensor moments [84]. The total value is $\kappa_T^{u-d} = 1.97$, which is larger than the light-front constituent quark model estimates. Using a harmonic-oscillator wave function (HO), Ref. [68] obtained $\kappa_T^{u-d} = 1.24$, while the hypercentral potential (HYP) gives $\kappa_T^{u-d} = 0.81$. This difference is not unexpected, since constituent quark models are based primarily on valence degrees of freedom, whereas the present calculation contains a sizable contribution from the polarized Dirac sea. Lattice QCD gives $\kappa_T^{u-d} = 1.051 \pm 0.094$ [55], which is substantially smaller than our result. The difference may reflect several systematic effects, including the model scale of the χQSM and the truncation of the $1/N_c$ expansion. In addition, a direct comparison with lattice QCD requires the tensor operator to be matched at the same renormalization scale. We therefore regard this comparison as qualitative. Finally, the light-cone QCD sum-rule calculation of Ref. [101] gives $\kappa_T^{u-d} = 1.82$, which is in close agreement with our total value.

The isoscalar tensor quadrupole moment receives a discrete-level contribution of $E_T^{u+d}(0)[\mathrm{lev}] = 5.66$ and a Dirac-sea contribution of $E_T^{u+d}(0)[\mathrm{sea}] = 0.32$. The sea contribution is therefore about 5.5% of the discrete-level contribution, showing that $E_T^{u+d}(0)$ is dominated by the valence level. The total value is $E_T^{u+d}(0) = 5.98$. This behavior differs from that of the isovector tensor quadrupole moment, for which the Dirac-sea contribution amounts to almost half of the total value [75]. This valence dominance allows a direct comparison with quark-model calculations. In particular, a recent bag-model study [70] also finds a positive value for $E_T(0)$, although its magnitude is smaller than ours. Since the tensor charge, corresponding to the monopole component, is of comparable size in the two approaches, the larger difference in the quadrupole moment is likely related to its stronger sensitivity to the relativistic structure of the quark wave functions. As shown in our previous work [75], the tensor charge is dominated by the large (nonrelativistic) component, while the small (relativistic) component gives only a subleading correction. By contrast, the tensor quadrupole moment is more sensitive to the small component. The difference from the bag-model result therefore reflects the different relativistic dynamics realized in the two approaches.

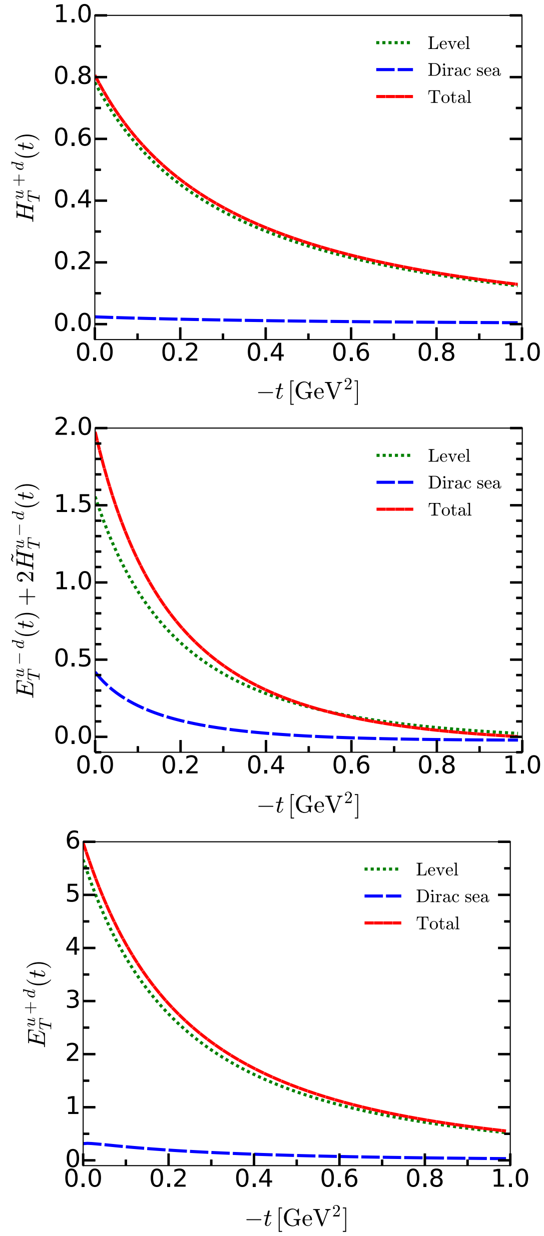

FIG. 1. The t dependence of the tensor form factors $(H_T^{u+d}, E_T^{u-d} + 2\tilde{H}_T^{u-d}, E_T^{u+d})$. Solid curves: total contributions, including the discrete-level and Dirac-sea parts. Dashed curves: Dirac-sea contributions. Dotted curves: discrete-level contributions.

The tensor multipole moments are given by the forward limits of the tensor form factors, while their t dependence provides additional information on the nucleon structure. We therefore evaluate the tensor form factors using Eq. (36). Since the large-N_c expansion is reliable only for $|t| \ll M_N^2$, we restrict ourselves to $|t| \lesssim 1\ \mathrm{GeV}^2$. The numerical results are displayed in Fig. 1, where the solid curves show the total results, while the dotted and dashed ones correspond to the discrete-level and Dirac-sea contributions, respectively.

The Dirac-sea contributions to H_T^{u+d} and E_T^{u+d} decrease monotonically with increasing $-t$ and remain much smaller than the corresponding discrete-level contributions. These form factors are therefore largely governed by the valence level. By contrast, the Dirac-sea contribution to $E_T^{u-d} + 2\tilde{H}_T^{u-d}$ exhibits a pronounced falloff already in the small-$|t|$ region and is sizable compared with the sea contributions to H_T^{u+d} and E_T^{u+d}. This indicates that the polarized Dirac sea plays a non-negligible role in the dipole structure.

VI. SUMMARY AND CONCLUSIONS

In this work, we have investigated the multipole structure of nucleon tensor form factors within the framework of the chiral quark-soliton model. This work extends our previous leading-order study in the $1/N_c$ expansion, in which the dominant tensor multipole form factors were obtained. In the leading-order treatment, the classical nucleon is described by a static pion mean field. Owing to the spin-flavor symmetry of this mean field, only selected isospin combinations contribute to the tensor multipole form factors. Thus, while the leading-order result captures the dominant structures, it does not complete the flavor decomposition. To obtain the missing flavor components, one has to include the collective rotational motion of the classical nucleon. These rotations generate the rotational $1/N_c$ corrections, which provide the first nonvanishing contributions to the isospin components that are absent at leading order. In the present work, we computed these contributions explicitly and thereby obtained the subleading tensor multipole form factors. We then examined the numerical size of these contributions through the tensor multipole moments. The resulting values are $g_T^{u+d} = 0.81$, $\kappa_T^{u-d} = 1.97$, and $E_T^{u+d}(0) = 5.98$. By separating the discrete-level and Dirac-sea contributions, we found that the isoscalar tensor charge g_T^{u+d} and the isoscalar tensor quadrupole moment $E_T^{u+d}(0)$ are largely dominated by the discrete level. This explains why these observables are close to the quark-model picture based mainly on valence-quark degrees of freedom. The isovector anomalous tensor magnetic moment κ_T^{u-d}, however, exhibits a different behavior. It receives a sizable Dirac-sea contribution, indicating that sea-quark effects are more relevant for the isovector tensor dipole structure than for the isoscalar monopole and quadrupole moments. This pattern is also reflected in the momentum-transfer dependence of the corresponding tensor form factors. In the region considered here, all three form factors decrease monotonically as $-t$ increases. Among them, the isovector anomalous tensor magnetic form factor, $E_T^{u-d}(t) + 2\tilde{H}_T^{u-d}(t)$, exhibits a particularly rapid falloff in the small-$|t|$ region. This behavior is consistent with its sizable Dirac-sea contribution and further supports the importance of sea-quark effects in the isovector tensor dipole structure.

As a future direction, the present framework can be extended in several ways. First, the rotational $1/N_c$ expansion also induces corrections to the leading tensor form factors themselves. Although these contributions are subleading, they are needed to complete the flavor decomposition of the tensor multipole form factors in a consistent manner at the same order in the $1/N_c$ expansion. Their numerical evaluation, however, requires a careful treatment of the spectral sums over the quark single-particle states. In particular, the rotational $1/N_c$ correction to the isovector tensor quadrupole form factor is highly sensitive to finite-box effects in the Kahana-Ripka basis, which makes its numerical convergence difficult to control. We therefore leave a systematic calculation of this correction for future work. Second, the present framework can be generalized to flavor SU(3) symmetry. Such an extension would allow us to include the strange-quark contribution and thereby complete the flavor decomposition beyond the two-flavor sector. It would also make it possible to investigate the tensor form factors of the lowest-lying hyperons within the same theoretical framework. Finally, the Δ baryon appears as a rotationally excited state of the classical nucleon and can be treated on the same footing as the nucleon. The study of the Δ tensor form factors would therefore provide access to a richer tensor structure and clarify how the tensor multipole patterns change under rotational excitation.

ACKNOWLEDGMENTS

H.-Ch. K. is grateful to Cédric Lorcé for valuable discussion and hospitality during his visit to Le Centre de Physique Théorique (CPHT) at École polytechnique, where part of the present work was done. The work was supported by the Basic Science Research Program through the National Research Foundation of Korea funded by the Korean government (Ministry of Education, Science and Technology, MEST), Grant No. RS-2025-00513982. H.-Y. W. acknowledges France Excellence scholarship through Campus France funded by the French government (Ministère de l’Europe et des Affaires Étrangères), Grant No. 141295X. N.-Y. Gh. received funding from the Basic Science Research Program of the National Research Foundation of Korea, funded by the Korean government (Ministry of Education, Science and Technology, MEST), under Grant No. RS-2025-25430144.

DATA AVAILABILITY

There are no publicly available research data or software supporting this manuscript. Requests for further information or data should be sent to the authors.

APPENDIX: 3D TENSOR MULTIPOLE DISTRIBUTIONS

In this appendix, we give the explicit expressions for the spatial distributions introduced in Eq. (37) in terms of irreducible matrix elements:

$$\rho_{T0}^{u+d}(r) = -\frac{N_c}{6I}\left(\sum_{E_n\neq E_{\rm lev}}\frac{\langle {\rm lev}||\tau_1||n\rangle}{E_{\rm lev}-E_n}\langle n||r\rangle\{O_{T0}\}_1\langle r||{\rm lev}\rangle + \sum_{n,m}R_3^{nm}\langle n||\tau_1||m\rangle\langle m||r\rangle\{O_{T0}\}_1\langle r||n\rangle\right), \tag{A1a}$$

$$\rho_{T1}^{u-d}(r) = -\frac{iM_{\rm cl}N_c}{3\sqrt{3}I}\left(\sum_{E_n\neq E_{\rm lev}}\frac{\langle {\rm lev}||\tau_1||n\rangle}{E_{\rm lev}-E_n}\times\langle n||r\rangle\{O_{T1}\}_1\langle r||{\rm lev}\rangle + \sum_{n,m}R_3^{nm}\langle n||\tau_1||m\rangle\times\langle m||r\rangle\{O_{T1}\}_1\langle r||n\rangle\right), \tag{A1b}$$

$$\rho_{T2}^{u+d}(r) = -\frac{2M_{\rm cl}^2N_c}{15I}\left(\sum_{E_n\neq E_{\rm lev}}\frac{\langle {\rm lev}||\tau_1||n\rangle}{E_{\rm lev}-E_n}\times\langle n||r\rangle\{O_{T2}\}_1\langle r||{\rm lev}\rangle + \sum_{n,m}R_3^{nm}\langle n||\tau_1||m\rangle\times\langle m||r\rangle\{O_{T2}\}_1\langle r||n\rangle\right). \tag{A1c}$$

Here, the first term in each expression is the discrete-level contribution, while the second term is the Dirac-sea contribution. The Dirac-sea contribution is regularized by the function R_3^{nm} in the proper-time regularization scheme, with the cutoff mass Λ given in Eq. (39). The explicit form of R_3^{nm} is

$$R_3^{nm} = \frac{1}{2\sqrt{\pi}}\int_{1/\Lambda^2}^{\infty}\frac{du}{\sqrt{u}}\left[\frac{e^{-uE_n^2}-e^{-uE_m^2}}{u(E_m^2-E_n^2)} - \frac{E_ne^{-uE_n^2}+E_me^{-uE_m^2}}{E_m-E_n}\right]. \tag{A2}$$

The operators $\{O_{T0}\}_1$, $\{O_{T1}\}_1$, and $\{O_{T2}\}_1$ appearing in the spatial distributions have the following explicit forms:

$$\{O_{T0}\}_1 = \Sigma_1\gamma^0, \tag{A3a}$$

$$\{O_{T1}\}_1 = [[4\pi rY_1\otimes\gamma_1]_0\otimes\tau]_1, \tag{A3b}$$

$$\{O_{T2}\}_1 = [4\pi r^2Y_2\otimes\Sigma_1]_1\gamma_0. \tag{A3c}$$

[1] S. L. Adler, E. W. Colglazier, Jr., J. B. Healy, I. Karliner, J. Lieberman, Y. J. Ng, and H.-S. Tsao, Phys. Rev. D **11**, 3309 (1975).
[2] R. L. Jaffe and X.-D. Ji, Phys. Rev. Lett. **67**, 552 (1991).
[3] R. L. Jaffe and X.-D. Ji, Nucl. Phys. **B375**, 527 (1992).
[4] H.-x. He and X.-D. Ji, Phys. Rev. D **52**, 2960 (1995).
[5] J. Erler and M. J. Ramsey-Musolf, Prog. Part. Nucl. Phys. **54**, 351 (2005).
[6] M. Pospelov and A. Ritz, Ann. Phys. (Amsterdam) **318**, 119 (2005).
[7] N. Severijns, M. Beck, and O. Naviliat-Cuncic, Rev. Mod. Phys. **78**, 991 (2006).
[8] V. Cirigliano, S. Gardner, and B. Holstein, Prog. Part. Nucl. Phys. **71**, 93 (2013).
[9] A. Courtoy, S. Baeßler, M. González-Alonso, and S. Liuti, Phys. Rev. Lett. **115**, 162001 (2015).
[10] T. Bhattacharya, V. Cirigliano, S. D. Cohen, R. Gupta, A. Joseph, H.-W. Lin, and B. Yoon (Precision Neutron Decay Matrix Elements (PNDME) Collaboration), Phys. Rev. D **92**, 094511 (2015).
[11] M. González-Alonso, O. Naviliat-Cuncic, and N. Severijns, Prog. Part. Nucl. Phys. **104**, 165 (2019).
[12] C. Antel *et al.*, Eur. Phys. J. C **83**, 1122 (2023).
[13] J. Goodman, M. Ibe, A. Rajaraman, W. Shepherd, Tim M. P. Tait, and H.-B. Yu, Phys. Rev. D **82**, 116010 (2010).
[14] F. Bishara, J. Brod, B. Grinstein, and J. Zupan, J. High Energy Phys. 11 (2017) 059.
[15] J. Brod, A. Gootjes-Dreesbach, M. Tammaro, and J. Zupan, J. High Energy Phys. 10 (2018) 065; 07 (2023) 012(E).
[16] K. Ma, Phys. Dark Universe **50**, 102090 (2025).
[17] A. Glick-Magid, Phys. Rev. D **110**, L051701 (2024).
[18] J.-H. Liang, Y. Liao, X.-D. Ma, and H.-L. Wang, Phys. Rev. D **111**, 095033 (2025).
[19] J. P. Ralston and D. E. Soper, Nucl. Phys. **B152**, 109 (1979).

[20] J. Kodaira, S. Matsuda, K. Sasaki, and T. Uematsu, Nucl. Phys. **B159**, 99 (1979).
[21] X. Artru and M. Mekhfi, Z. Phys. C **45**, 669 (1990).
[22] A. P. Bukhvostov, E. A. Kuraev, and L. N. Lipatov, Sov. Phys. JETP **60**, 22 (1984).
[23] J. L. Cortes, B. Pire, and J. P. Ralston, Z. Phys. C **55**, 409 (1992).
[24] V. Barone, F. Bradamante, and A. Martin, Prog. Part. Nucl. Phys. **65**, 267 (2010).
[25] C. A. Aidala, S. D. Bass, D. Hasch, and G. K. Mallot, Rev. Mod. Phys. **85**, 655 (2013).
[26] S. Diehl, Prog. Part. Nucl. Phys. **133**, 104069 (2023).
[27] L. W. Whitlow, E. M. Riordan, S. Dasu, S. Rock, and A. Bodek, Phys. Lett. B **282**, 475 (1992).
[28] J. Kodaira, Prog. Theor. Phys. Suppl. **120**, 37 (1995).
[29] A. V. Efremov, K. Goeke, and P. Schweitzer, Eur. Phys. J. C **35**, 207 (2004).
[30] V. Barone *et al.* (PAX Collaboration), arXiv:hep-ex/0505054.
[31] M. Anselmino, V. Barone, A. Drago, and N. N. Nikolaev, Phys. Lett. B **594**, 97 (2004).
[32] B. Pasquini, M. Pincetti, and S. Boffi, Phys. Rev. D **76**, 034020 (2007).
[33] A. Airapetian *et al.* (HERMES Collaboration), Phys. Rev. Lett. **94**, 012002 (2005).
[34] V. Y. Alexakhin *et al.* (COMPASS Collaboration), Phys. Rev. Lett. **94**, 202002 (2005).
[35] M. Anselmino, M. Boglione, U. D'Alesio, A. Kotzinian, F. Murgia, A. Prokudin, and C. Turk, Phys. Rev. D **75**, 054032 (2007).
[36] M. Anselmino, M. Boglione, U. D'Alesio, A. Kotzinian, F. Murgia, A. Prokudin, and S. Melis, Nucl. Phys. B, Proc. Suppl. **191**, 98 (2009).
[37] M. Anselmino, M. Boglione, U. D'Alesio, S. Melis, F. Murgia, and A. Prokudin, Phys. Rev. D **87**, 094019 (2013).
[38] Z.-B. Kang, A. Prokudin, P. Sun, and F. Yuan, Phys. Rev. D **91**, 071501(R) (2015).
[39] J. C. Collins, Nucl. Phys. **B396**, 161 (1993).
[40] R. Seidl *et al.* (Belle Collaboration), Phys. Rev. D **78**, 032011 (2008); **86**, 039905(E) (2012).
[41] M. Radici, A. Courtoy, A. Bacchetta, and M. Guagnelli, J. High Energy Phys. 05 (2015) 123.
[42] Z. Ye, N. Sato, K. Allada, T. Liu, J.-P. Chen, H. Gao, Z.-B. Kang, A. Prokudin, P. Sun, and F. Yuan, Phys. Lett. B **767**, 91 (2017).
[43] H.-W. Lin, W. Melnitchouk, A. Prokudin, N. Sato, and H. Shows, Phys. Rev. Lett. **120**, 152502 (2018).
[44] C. Cocuzza, A. Metz, D. Pitonyak, A. Prokudin, N. Sato, and R. Seidl (JAM Collaboration), Phys. Rev. Lett. **132**, 091901 (2024).
[45] C. Cocuzza, A. Metz, D. Pitonyak, A. Prokudin, N. Sato, and R. Seidl (Jefferson Lab Angular Momentum (JAM) Collaboration), Phys. Rev. D **109**, 034024 (2024).
[46] M.-S. Gao, Z.-B. Kang, W. Li, and D. Y. Shao, Phys. Rev. Lett. **136**, 151902 (2026).
[47] S. Aoki, M. Doui, T. Hatsuda, and Y. Kuramashi, Phys. Rev. D **56**, 433 (1997).
[48] M. Göckeler, P. Hägler, R. Horsley, Y. Nakamura, D. Pleiter, P. E. L. Rakow, A. Schäfer, G. Schierholz, H. Stüben, and J. M. Zanotti (QCDSF Collaboration and UKQCD Collaboration), Phys. Rev. Lett. **98**, 222001 (2007).
[49] C. Alexandrou *et al.*, Phys. Rev. D **95**, 114514 (2017); **96**, 099906(E) (2017).
[50] R. Gupta, B. Yoon, T. Bhattacharya, V. Cirigliano, Y.-C. Jang, and H.-W. Lin, Phys. Rev. D **98**, 091501(R) (2018).
[51] N. Yamanaka, S. Hashimoto, T. Kaneko, and H. Ohki (JLQCD Collaboration), Phys. Rev. D **98**, 054516 (2018).
[52] C. Alexandrou, S. Bacchio, M. Constantinou, J. Finkenrath, K. Hadjiyiannakou, K. Jansen, G. Koutsou, and A. Vaquero Aviles-Casco, Phys. Rev. D **102**, 054517 (2020).
[53] C. Alexandrou, M. Constantinou, K. Hadjiyiannakou, K. Jansen, and F. Manigrasso, Phys. Rev. D **104**, 054503 (2021).
[54] S. Park, R. Gupta, B. Yoon, S. Mondal, T. Bhattacharya, Y.-C. Jang, B. Joó, and F. Winter (Nucleon Matrix Elements (NME) Collaboration), Phys. Rev. D **105**, 054505 (2022).
[55] C. Alexandrou, S. Bacchio, M. Constantinou, P. Dimopoulos, J. Finkenrath, R. Frezzotti, K. Hadjiyiannakou, K. Jansen, B. Kostrzewa, G. Koutsou, G. Spanoudes, and C. Urbach, Phys. Rev. D **107**, 054504 (2023).
[56] M. Rodekamp, M. Engelhardt, J. R. Green, S. Krieg, S. Liuti, S. Meinel, J. W. Negele, A. Pochinsky, and S. Syritsyn, Phys. Rev. D **109**, 074508 (2024).
[57] J.-H. Wang, Z.-C. Hu, X. Ji, X. Jiang, Y. Su, P. Sun, and Y.-B. Yang, arXiv:2511.02326.
[58] X.-D. Ji, J. Phys. G **24**, 1181 (1998).
[59] M. Diehl, Eur. Phys. J. C **19**, 485 (2001).
[60] K. Goeke, M. V. Polyakov, and M. Vanderhaeghen, Prog. Part. Nucl. Phys. **47**, 401 (2001).
[61] M. Diehl, Phys. Rep. **388**, 41 (2003).
[62] A. V. Belitsky and A. V. Radyushkin, Phys. Rep. **418**, 1 (2005).
[63] S. Boffi and B. Pasquini, Riv. Nuovo Cimento **30**, 387 (2007).
[64] K. Kumericki, S. Liuti, and H. Moutarde, Eur. Phys. J. A **52**, 157 (2016).
[65] N. d'Hose, S. Niccolai, and A. Rostomyan, Eur. Phys. J. A **52**, 151 (2016).
[66] M. Burkardt, Phys. Rev. D **72**, 094020 (2005).
[67] M. Diehl and P. Hägler, Eur. Phys. J. C **44**, 87 (2005).
[68] B. Pasquini, M. Pincetti, and S. Boffi, Phys. Rev. D **72**, 094029 (2005).
[69] C. Lorce, B. Pasquini, and M. Vanderhaeghen, J. High Energy Phys. 05 (2011) 041.
[70] K. Tezgin, B. Maynard, and P. Schweitzer, Phys. Rev. D **110**, 054028 (2024).
[71] S. Kaur, S. Xu, C. Mondal, X. Zhao, and J. P. Vary (BLFQ Collaboration), Phys. Rev. D **109**, 014015 (2024).
[72] N. Kaur and H. Dahiya, Phys. Rev. D **112**, 074024 (2025).
[73] X. Luan and Z. Lu, Phys. Rev. D **110**, 034021 (2024).
[74] T. M. Aliev, K. Azizi, and M. Savci, Phys. Rev. D **84**, 076005 (2011).
[75] N.-Y. Ghim, H.-Y. Won, J.-Y. Kim, and H.-C. Kim, Phys. Rev. D **111**, 074024 (2025).
[76] H.-C. Kim, M. V. Polyakov, and K. Goeke, Phys. Rev. D **53**, R4715 (1996).

[77] H.-C. Kim, M. V. Polyakov, and K. Goeke, Phys. Lett. B **387**, 577 (1996).
[78] M. Wakamatsu, Phys. Rev. D **79**, 014033 (2009).
[79] C. Lorce, Phys. Rev. D **79**, 074027 (2009).
[80] T. Ledwig, A. Silva, and H.-C. Kim, Phys. Rev. D **82**, 054014 (2010).
[81] T. Ledwig, A. Silva, and H.-C. Kim, Phys. Rev. D **82**, 034022 (2010).
[82] T. Ledwig and H.-C. Kim, Phys. Rev. D **85**, 034041 (2012).
[83] J.-Y. Kim and C. Weiss, Phys. Rev. D **111**, 074007 (2025).
[84] J.-Y. Kim, Phys. Rev. D **112**, 074032 (2025).
[85] C. G. Callan, Jr., R. F. Dashen, and D. J. Gross, Phys. Rev. D **17**, 2717 (1978).
[86] R. D. Carlitz and D. B. Creamer, Ann. Phys. (Amsterdam) **118**, 429 (1979).
[87] E. V. Shuryak, Nucl. Phys. **B203**, 93 (1982).
[88] D. Diakonov and V. Y. Petrov, Nucl. Phys. **B272**, 457 (1986).
[89] T. Schäfer and E. V. Shuryak, Rev. Mod. Phys. **70**, 323 (1998).
[90] D. Diakonov, Prog. Part. Nucl. Phys. **51**, 173 (2003).
[91] D. Diakonov, V. Y. Petrov, and P. V. Pobylitsa, Nucl. Phys. **B306**, 809 (1988).
[92] E. Witten, Nucl. Phys. **B160**, 57 (1979).
[93] E. Witten, Nucl. Phys. **B223**, 422 (1983).
[94] C. V. Christov, A. Blotz, H.-C. Kim, P. Pobylitsa, T. Watabe, T. Meissner, E. Ruiz Arriola, and K. Goeke, Prog. Part. Nucl. Phys. **37**, 91 (1996).
[95] G.-S. Yang, H.-C. Kim, M. V. Polyakov, and M. Praszałowicz, Phys. Rev. D **94**, 071502(R) (2016).
[96] H.-C. Kim, J. Korean Phys. Soc. **73**, 165 (2018).
[97] J.-Y. Kim and H.-C. Kim, Prog. Theor. Exp. Phys. **2020**, 043D03 (2020).
[98] J.-M. Suh, J.-Y. Kim, G.-S. Yang, and H.-C. Kim, Phys. Rev. D **106**, 054032 (2022).
[99] S. Kahana and G. Ripka, Nucl. Phys. **A429**, 462 (1984).
[100] M. Wakamatsu, Phys. Lett. B **653**, 398 (2007).
[101] G. Erkol and A. Ozpineci, Phys. Lett. B **704**, 551 (2011).